

Thermoelectricity of Molecular tunnel Junctions

Yu-Shen Liu and Yu-Chang Chen*

Department of Electrophysics, National Chiao Tung University, 1001 Ta Hsueh Road, Hsinchu 30010, Taiwan

A first-principles approach is presented for the thermoelectricity in molecular junctions formed by a single molecule contact. The study investigates the Seebeck coefficient considering the source-drain electrodes with distinct temperatures and chemical potentials in a three-terminal geometry junction. We compare the Seebeck coefficient in the amino-substituted and unsubstituted butanethiol junction and observe interesting thermoelectric properties in the amino-substituted junction. Due to the novel states around the Fermi levels introduced by the amino-substitution, the Seebeck coefficient could be easily modulated by using gate voltages and biases. When the temperature in one of the electrodes is fixed, the Seebeck coefficient varies significantly with the temperature in the other electrode, and such dependence could be modulated by varying the gate voltages. As the biases increase, richer features in the Seebeck coefficient are observed, which are closely related to the transmission functions in the vicinity of the left and right Fermi levels.

Building electronic circuits from molecules is an inspiring idea [1, 2, 3, 4]. Much attention has been devoted to investigating the various transport properties that might be applicable in developing new forms of electronic and energy-conversion devices, such as electron transfer [5, 6], shot noise [7], heat transport [8, 9], negative differential resistance [10], and gate-controlled effects [11]. Recently, topics on thermo-related transport, such as local heating [9, 12, 13] and thermal transport [14], have emerged as new subfields in molecular electronics. Another important thermo-related property in the molecular tunnel junction (m-M-m) is thermoelectricity [15, 16, 17, 18, 19, 20, 21, 22, 23]. The Seebeck coefficient, which is related not only to the magnitude but also to the slope of the transmission function in the vicinity of Fermi levels, can provide more information than current-voltage characteristics. The study of thermoelectricity is of key importance in the design of novel thermo-related electronic and nanoscale energy conversion devices.

Recent experimental measurements of the Seebeck coefficient for molecular tunnel junctions were conducted at zero bias [21, 23]. In such cases, the system can be described by only a single Fermi level. Similarly, the Seebeck coefficient for bulk material is also described by a single Fermi level. Nevertheless, molecular tunnel junctions consist of two electrodes as independent electron and heat reservoirs. Thus, it is worthwhile extending the investigation of the Seebeck coefficients to a system with distinct temperatures ($T_{L(R)}$) and chemical potentials ($\mu_{L(R)}$) in the left (right) electrode. In this letter, we present a theory for two distinct Fermi levels in molecular tunnel junction combining a first-principles approach for the Seebeck coefficient in the two- and three-terminal junctions in nonlinear regime. As an example, we systematically investigate the dependence of the Seebeck coefficient on the source-drain biases, gate voltages, and temperatures in the metal electrodes before and after amino-substitution in the butanethiol molecular junction. The Seebeck coefficient may provide further insights into the physical properties of molecular tunnel junctions. For

example, whether the Fermi energy is closer to the lowest unoccupied molecular orbital (LUMO) or the highest occupied molecular orbital (HOMO) may be locally probed via thermoelectricity measurements [16]. Interesting features in the Seebeck coefficient are observed in the amino-substituted butanethiol junction because of the dramatic change in the transmission functions by amino-substitution in the vicinity of the left and right Fermi levels.

Alkanethiol [$\text{CH}_3(\text{CH}_2)_{n-1}\text{SH}$, denoted as C_n]-related molecules are a good representation of reproducible junctions that can be fabricated [2, 3, 24]. It has been established that non-resonant tunneling is the main conduction mechanism inasmuch as the Fermi levels of the two electrodes lie within the large HOMO-LUMO gap. However, functional group substitution may have significant effects on the electronic structures of alkanethiols. New states around the Fermi levels are produced when $-\text{NH}_2$ is substituted for $-\text{H}$ in bridging butanethiol (C_4). The response of these states to external biases depends on the polarity and it leads to asymmetric current-voltage characteristics [25]. Because of the dramatic change in the transmission function in the vicinity of the Fermi levels, the novel characteristics of the Seebeck coefficient are observed in the amino-substituted junction. Consequently, the amino-substitution significantly affects the Seebeck coefficient. For example, the Seebeck coefficient can change signs by applying gate voltages and biases in the amino-substituted junction but not in the unsubstituted system. The influence of different temperatures between the two electrodes on the Seebeck coefficient, controllable by the gate voltages, is significant in the amino-substituted junction. The results suggest that the thermoelectric molecule devices, such as a molecular thermometer, are possible in the future.

Let us start by considering a single molecule sandwiched between two bulk electrodes applied with a certain source-drain bias. The Fermi level in the left/right electrodes is determined by filling the conduction band with the valence electrons in the bulk Au electrode de-

scribed by the jellium model ($r_s \approx 3$). The gate voltage is introduced as a capacitor composed of two parallel circular charged disks separated by a certain distance from each other [11, 27]. The axis of the capacitor is perpendicular to the transport direction. One plate is placed close to the molecule, while the other plate, placed far away from the molecule, is set to be the zero reference energy [Inset in Figure 1(a)]. Using the second-quantization field-operator technique with the effective single-particle wave functions calculated self-consistently in density functional theory, the current is given by [26]:

$$I = \frac{1}{\pi} \int dE [f_E^R(\mu_R, T_R)\tau^R(E) - f_E^L(\mu_L, T_L)\tau^L(E)], \quad (1)$$

where the transmission function of electron with energy E incident from the left (right) electrode is:

$$\tau^{L(R)}(E) = \pm i\pi \int d\mathbf{R} \int d\mathbf{K}_{\parallel} I_{EE}^{LL(RR)}(\mathbf{r}, \mathbf{K}_{\parallel}), \quad (2)$$

where $I_{EE}^{ij} = [\Psi_E^i]^* \nabla \Psi_{E'}^j - \nabla [\Psi_E^i]^* \Psi_{E'}^j$, and $i, j = L, R$. $\Psi_E^{L(R)}(\mathbf{r}, \mathbf{K}_{\parallel})$ is the single-particle wave function (detailed theory can be found in Ref. [26, 28]) incident from

the left (right) electrode with energy E and component of the momentum \mathbf{K}_{\parallel} parallel to the electrode surface, and $d\mathbf{R}$ represents an element of the electrode surface. The stationary wave function $\Psi_E^{L(R)}(\mathbf{r}, \mathbf{K}_{\parallel})$ can be calculated by solving the Lippmann-Schwinger equation iteratively to self-consistency [28, 29, 30]. The exchange-correlation potential is included in density-functional formalism by using the local-density approximation [31]. Once the single-particle wave functions are calculated self-consistently, the transmission function of electron with energy E can be calculated using Eq. (2). We assume that the left (right) electrode serves as the electron and thermal reservoir with the electron population described by the Fermi-Dirac distribution function, $f_E^{L(R)} = 1 / (\exp((E - \mu_{L(R)}) / k_B T_{L(R)}) + 1)$, where $\mu_{L(R)}$ and $T_{L(R)}$ are the chemical potential and the temperature in the left (right) electrode, respectively, and k_B is the Boltzmann constant.

This research considers the extra current induced by an additional infinitesimal temperature (ΔT) and voltage (ΔV) distributed symmetrically across the molecular junction:

$$\Delta I = I(\mu_L, T_L + \frac{\Delta T}{2}; \mu_R, T_R - \frac{\Delta T}{2}) + I(\mu_L + \frac{e\Delta V}{2}, T_L; \mu_R - \frac{e\Delta V}{2}, T_R) - 2I(\mu_L, T_L; \mu_R, T_R), \quad (3)$$

The Seebeck coefficient (defined as $S = \frac{\Delta V}{\Delta T}$) is obtained by letting $\Delta I = 0$. We expand the Fermi-Dirac distribution function to the first order in ΔT and ΔV and obtain

$$S = -\frac{1}{e} \frac{\frac{K_1^L}{T_L} + \frac{K_1^R}{T_R}}{\frac{K_0^L}{T_L} + \frac{K_0^R}{T_R}}, \quad (4)$$

where

$$K_n^{L(R)} = - \int dE (E - \mu_{L(R)})^n \frac{\partial f_E^{L(R)}}{\partial E} \tau(E), \quad (5)$$

and $\tau(E) = \tau^R(E) = \tau^L(E)$, a direct consequence of the time-reversal symmetry.

The research explores the dependence of the Seebeck coefficient on the gate voltages, temperatures in the electrodes, and the source-drain biases in both the linear and nonlinear response regimes by applying Eq. (4). In the low-temperature regime where the higher order terms in the temperature are disregarded, Eq. (4) can be simplified using the Sommerfeld expansion [19, 20, 32]:

$$S = -\frac{\pi^2 k_B^2}{3e} \frac{T_L \frac{\partial \tau(E)}{\partial E} |_{E=\mu_L} + T_R \frac{\partial \tau(E)}{\partial E} |_{E=\mu_R}}{\tau(\mu_L) + \tau(\mu_R)}, \quad (6)$$

where the Seebeck coefficient is closely related to the transmission function in the vicinity of the left and right Fermi levels.

As the first step in our analysis, we study the Seebeck coefficient in a three-terminal geometry in the linear response regime ($V_{SD} = 0.01$ V and $\mu_L \approx \mu_R \approx E_F$), where both electrodes have the same temperatures ($T_L = T_R = T$). In this case, the Seebeck coefficient can be simplified as $S = -\frac{1}{eT} \frac{\int (E - E_F) \frac{\partial f_E}{\partial E} \tau(E) dE}{\int \frac{\partial f_E}{\partial E} \tau(E) dE}$. In the low temperature regime, the Seebeck coefficient can be further simplified using the Sommerfeld expansion as $S = -\frac{\pi^2 k_B^2 T}{3e} \frac{\partial \ln \tau(E)}{\partial E} |_{E=E_F}$ [9, 16, 22]. This equation has been applied to the study of several atomic and molecular systems [19, 21]. The Seebeck coefficient as a function of the gate voltage for various temperatures in the amino-substituted and unsubstituted butanethiol junction is presented in Fig. 1(a). The results show that the characteristics of the Seebeck coefficient are sensitive to the gate voltages in the amino-substituted butanethiol junction. The most striking feature is that the molecular transistor can be converted from n-type to p-type by applying the gate voltages. The Seebeck coefficient is close to zero at $V_G \approx -2.6$ V. As the gate voltage further decreases, the sign of the Seebeck coefficient be-

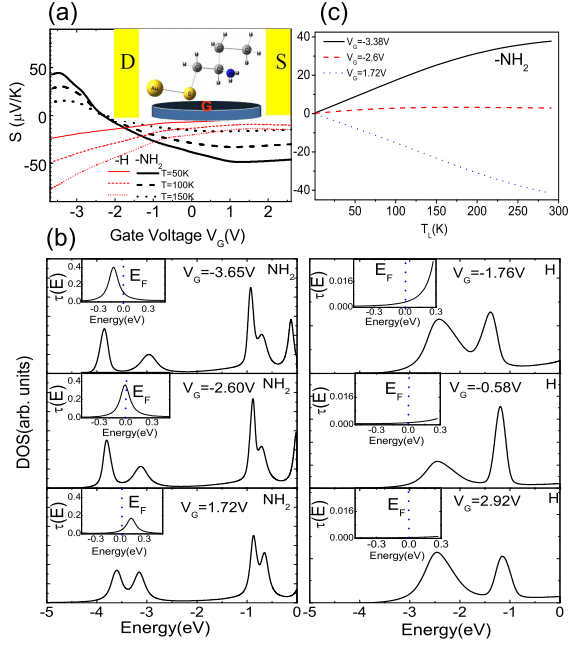


FIG. 1: (color online) The Seebeck coefficient S in a three-terminal geometry with $V_{SD} = 0.01V$: (a) The S versus V_G where $T_L = T_R = T$ for the amino-substituted [black (thick) lines] and unsubstituted [red (thin) lines] butanethiol for $T = 50$ K (solid line), $T = 100$ K (dashed line), and $T = 150$ K (dotted line). The inset shows the schematic of the three-terminal junction. The gate field is applied in a direction perpendicular to direction of charge transport. (b) The density of states and the transmission function (inset): the left panels for the amino-substituted butanethiol junction at $V_G = -3.65$, -2.60 , and 1.72 V; the right panels for the unsubstituted butanethiol junction at $V_G = -1.76$, -0.58 , and 2.92 V. (c) The S versus T_L for an amino-substituted butanethiol junction for $V_G = -3.38$, -2.60 , and 1.72 V, where $T_R = 0$ K.

comes positive (p-type). For the butanethiol molecular junction, the characteristic of the carrier remains n-type all the time because the sign of the Seebeck coefficient is negative.

To arrive at the physical reason why the gate voltage can efficiently modulate the Seebeck coefficient, the DOSs (transmission functions) are plotted as a function of energy for the various gate voltages in Fig. 1(b) (Inset of Fig. 1(b)). We observe that the positive (negative) gate voltage shifts the LUMO peak towards higher (lower) energies. At $V_G = -2.6$ V, the peak position of the LUMO and transmission function align with the Fermi levels, implying that $\partial \ln \tau(E)/\partial E|_{E=E_F} \approx 0$. Hence, the Seebeck coefficient is close to zero at the gate voltage around $V_G = -2.6$ V. When the gate voltage is tuned at around $V_G = 1.72$ V, the Seebeck coefficient is negative because $\partial \ln \tau(E)/\partial E|_{E=E_F} > 0$. Conversely, the Seebeck coefficient is positive because $\partial \ln \tau(E)/\partial E|_{E=E_F} < 0$ at $V_G = -3.65$ V. Thus, the characteristic of the carrier type of a certain molecular junction can be converted from n-type (closer to LUMO)

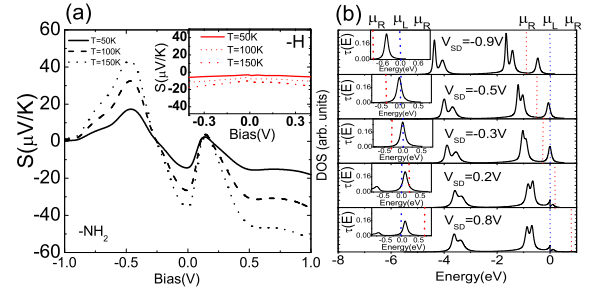


FIG. 2: (color online) (a) The Seebeck coefficient S as a function of source-drain biases in a two-terminal geometry for amino-substituted (the main graph) and unsubstituted (the inset in the upper right corner) butanethiol for $T = 50$ K (solid lines), $T = 100$ K (dashed lines), and $T = 150$ K (dotted lines). (b) The density of states and the transmission function (inset) for various source-drain biases ($V_{SD} = -0.9, -0.5, -0.3, 0.2, \text{ and } 0.8$ V) in the amino-substituted butanethiol junction.

to p-type (closer to HOMO) by tuning the gate voltage. In the unsubstituted butanethiol junction as shown in the right plane of Fig. 1(b), it is observed that the electron transmission function is always small because the location of the Fermi levels lies within the large HOMO-LUMO gap. We also note that the Seebeck coefficient has a negative value due to $\partial \ln \tau(E)/\partial E|_{E=E_F} > 0$. When the gate voltages are further decreased, the absolute value of the Seebeck coefficient becomes bigger even in the unsubstituted butanethiol junction because the negative gate voltage shifts the LUMO peak towards the lower energy region.

The Seebeck coefficient is relevant to the temperatures of the electrodes. This property may be applied to the design of a molecular thermometer. To show this, we investigate the Seebeck coefficient of the amino-substituted butanethiol junction at $V_{SD} = 0.01$ V as a function of temperature of the left electrode (T_L) while keeping $T_R = 0$ K as shown in Fig. 1(c). The results show that the dependence of the Seebeck coefficient on T_L is linear at low temperatures. In this regime, the Seebeck coefficient can be well described by Eq. (6), where $T_R = 0$ K. As the temperature T_L becomes large, the approximation of Eq. (6) turns out to be inappropriate, and the Seebeck coefficient shows nonlinear behavior. We further observe that the sensitivity of the Seebeck coefficient versus T_L can be amplified by applying gate voltages. At $V_G = -2.6$ V, the Seebeck coefficient has a very small value insensitive to T_L because the peak of the transmission function lies between two Fermi levels. When the gate voltage is tuned to $V_G = -3.38$ V, the Seebeck coefficient can be enhanced to around $38 \mu\text{V/K}$ at $T_L = 300$ K. The other interesting phenomenon observed is the possibility to change the sign of the Seebeck coefficient by applying the gate voltage. When the gate voltage is tuned to $V_G = 1.72$ V, the Seebeck coefficient becomes around $-42 \mu\text{V/K}$ at $T_L = 300$ K. The results

show that the amino-substituted butanethiol may be an effective thermoelectric material applicable to the design of molecular thermoelectric devices such as a thermometer.

The project further investigates the Seebeck coefficient in the nonlinear regime. The Seebeck coefficient of the amino-substituted (unsubstituted) butanethiol molecular junctions as a function of V_{SD} is plotted in Fig. 2(b) (Inset of Fig. 2(b)). At large V_{SD} , the difference between the left and right chemical potentials becomes significant. Thus, the transmission functions in the vicinity of both the left and right Fermi levels have important contribution to the Seebeck coefficient. In Fig. 2(b) we plot the DOSs and transmission functions as functions of the energy for various biases. For $V_{SD} > 0$, the states between the left and right Fermi levels are developed into a resonant peak similar to what is found in the elongated silicon point contact [33]. At large V_{SD} , the transmission functions around the left and right Fermi levels are equally important to the Seebeck coefficient (see Eq. (6)). When $T_L = T_R = T$, we explain the Seebeck coefficient in Fig. 2(a) by considering the source-drain bias V_{SD} at 0.8, -0.3 , and -0.5 V, respectively. For these biases, the contribution to the Seebeck coefficient is dominated by the transmission function in the vicinity of the left Fermi level. Thus, Eq. (6) can be further simplified as $S = -\frac{\pi^2 k_B^2 T}{3e} \frac{\partial \ln \tau(E)}{\partial E} |_{E=\mu_L}$. The Seebeck coefficient is (negative; zero; positive) at $V_{SD} = (0.8; -0.3; -0.5)$ V because $\partial \ln \tau(E)/\partial E |_{E=\mu_L}$ is ($>$; \approx ; $<$ 0). We also observe that there are more zeroes in the Seebeck coefficient as a function of V_{SD} in Fig. 2(a). For example at $V_{SD} = 0.2$ or -0.9 V, the peak position of the transmission function is located in the middle of the left and right Fermi levels such that $\partial \tau(E)/\partial E |_{E=\mu_L} \approx -\partial \tau(E)/\partial E |_{E=\mu_R}$. Consequently, the Seebeck coefficient is close to zero at $V_{SD} = 0.2$ and -0.9 V according to Eq. (6). In the unsubstituted butanethiol junction, the Seebeck coefficient as a function of V_{SD} is shown in the inset of Fig. 2(a). The results show that the Seebeck coefficient remains a negative value in the whole bias regime owing to the fact that the Fermi levels are located between the large HOMO-LUMO gap.

In conclusion, the study investigates the thermoelectricity in the molecular junction in both linear and nonlinear regimes. The Seebeck coefficients are studied using first-principles calculations. The general properties of the Seebeck effects can be very different for the unsubstituted and amino-substituted butanethiol junction in the two-terminal and three-terminal molecular geometries. The research illustrates that the gate field is able to modulate and optimize the Seebeck coefficient. Another interesting phenomenon is the possibility to change the signs of the Seebeck coefficient by applying the gate voltages and biases in amino-substituted butanethiol junction. It is observed that the Seebeck coefficient is relevant to the temperatures of the electrodes that may be applied to the design of a molecular thermometer, and its sensi-

bility can be controlled by gate voltages. We also extend the investigation of the Seebeck coefficient to molecular tunnel junction at finite biases. As the biases increase, richer features in the Seebeck coefficient are observed, which are closely related to the transmission functions in the vicinity of the left and right Fermi levels. All results show that the molecular tunnel junction based on alkanethiols may be a promising candidate for the design of novel thermoelectric devices in the future.

because $\partial \ln \tau(E)/\partial E |_{E=\mu_L}$ is

The authors thank MOE ATU, NCTS and NCHC for support under Grants NSC 97-2112-M-009-011-MY3, 097-2816-M-009-004, and 97-2120-M-009-005.

* Electronic address: yuchangchen@mail.nctu.edu.tw

- ¹ A. Aviram and M. A. Ratner, Chem. Phys. Lett. **29**, 277 (1974).
- ² C. H. Ahn, A. Bhattacharya, M. Di Ventra, J. N. Eckstein, C. D. Frisbie, M. E. Gershenson, A. M. Goldman, I. H. Inoue, J. Mannhart, A. J. Millis, A. F. Morpurgo, D. Natelson and J. M. Triscone, Rev. Mod. Phys. **78**, 1185 (2006).
- ³ S. M. Lindsay and M. A. Ratner, Advanced Materials **19**, 23(2007).
- ⁴ N. J. Tao, Nat. Nanotechnol. **1**, 173 (2006).
- ⁵ W. U. Huynh, J. J. Dittmer and A. P. Alivisatos, Science **295**, 2425 (2002).
- ⁶ A. Nitzan and M. A. Ratner, Science **300**, 1384 (2003).
- ⁷ X. Q. Shi, Z. X. Dai, G. H. Zhong, X. H. Zheng and Z. J. Zeng, Phys. Chem. C **111**, 10130 (2007).
- ⁸ A. Nitzan, Science **317**, 759 (2007).
- ⁹ M. Galperin, A. Nitzan and M. A. Ratner, Phys. Rev. B **75**, 155312 (2007).
- ¹⁰ J. Chen, M. A. Reed, A. M. Rawlett and J. M. Tour, Science **286**, 1550 (1999).
- ¹¹ M. Di Ventra, S. T. Pantelides and N. D. Lang, Appl. Phys. Lett. **76**, 3448 (2000).
- ¹² Z. F. Huang, B. Q. Xu, Y. C. Chen, M. Di Ventra and N. J. Tao, Nano Lett. **6**, 1240 (2006).
- ¹³ Z. F. Huang, F. Chen, R. D'Agosta, P. A. Bennett, M. Di Ventra and N. J. Tao, Nat. Nanotechnol. **2**, 698 (2007).
- ¹⁴ R. Prasher, T. Tong and A. Majumdar, Nano Lett. **8**, 99 (2008).
- ¹⁵ D. Yonatan and M. Di Ventra, Nano Lett. (in press).
- ¹⁶ M. Paulsson and S. Datta, Phys. Rev. B **67**, 241403(R) (2003).
- ¹⁷ F. Pauly, J. K. Viljas and J. C. Cuevas, Phys. Rev. B **78**, 035315 (2008).
- ¹⁸ D. Segal, J. Chem. Phys. **128**, 224710 (2008).
- ¹⁹ X. H. Zheng, W. Zheng, Y. D. Wei, Z. Zeng and J. Wang, Chem. Phys. **121**, 8537 (2004).
- ²⁰ B. Ludoph and J. M. van Ruitenbeek, Phys. Rev. B **59**, 12290 (1999).
- ²¹ P. Reddy, S. Y. Jang, R. A. Segalman and A. Majumdar, Science **315**, 1568 (2007).
- ²² M. Galperin, A. Nitzan and M. A. Ratner, Mol. Phys. **106**, 397 (2008).
- ²³ K. Baheti, J. A. Malen, P. Doak, P. Reddy, S. Y. Jang, T. D. Tilley, A. Majumdar and R. A. Segalman, Nano Lett. **8**, 715 (2008).

- ²⁴ N. J. Tao, Nat. Nanotechnol. **1**, 173 (2006).
- ²⁵ C. L. Ma, D. Nghiem and Y. C. Chen, Appl. Phys. Lett. **93**, 222111 (2008).
- ²⁶ Y. C. Chen and M. Di Ventra, Phys. Rev. B **67**, 153304 (2003).
- ²⁷ M. Di Ventra, S. T. Pantelides and N. D. Lang, Phys. Rev. Lett. **84**, 979 (2000).
- ²⁸ N. D. Lang, Phys. Rev. B **52**, 5335 (1995).
- ²⁹ M. Di Ventra, S. T. Pantelides and N. D. Lang, Appl. Phys. Lett. **76**, 3448 (2000).
- ³⁰ Z. Yang, A. Tackett and M. Di Ventra, Phys. Rev. B **66**, 041405(R) (2002).
- ³¹ P. Hohenberg and W. Kohn, Phys. Rev. B **136**, 864 (1964); W. Kohn and L.J. Sham, Phys. Rev. **140**, A1133 (1965).
- ³² B. Wang, Y. Xing, L. Wan, Y. Wei and J. Wang, Phys. Rev. B **71**, 233406 (2005).
- ³³ M. Di Ventra, Y. C. Chen and T. N. Todorov, Phys. Rev. Lett. **92**, 176803 (2004).